OXYGEN TRANSPORT PROCESSES IN THE NORDHALDE OF THE RONNENBURG MINING DISTRICT, GERMANY

Jason Smolensky, Daryl Hockley
Steffen, Robertson and Kirsten (Canada) Inc.
Suite 800, 580 Hornby Street, Vancouver, BC Canada V6C 3B6

René Lefebvre
INRS-Géoressources
2535 Laurier, Sainte-Foy, PQ, Canada G1V 4C7

Michael Paul
Engineering Department, Wismut GmbH
P.O. Box 52, D-09034 Chemnitz, Ronnenburg, Germany

ABSTRACT

The Nordhalde is one of the largest waste rock piles in the Ronnenburg uranium mining district (former East Germany), consisting of approximately 27 Mm^3 of material containing approximately 1-2% pyrite. To better understand the physical processes that control pyrite oxidation and acid generation within the pile, extensive drilling and geochemical characterisation were carried out and eight instrumented boreholes were installed in 1996. The boreholes were equipped to monitor the spatial distribution of oxygen, pressure and temperature within the pile. A qualitative analysis of a year of data from the boreholes showed that the active processes of oxygen transport in the pile include diffusion, barometric pumping and thermal convection. The oxygen and temperature data were used to determine independent, order of magnitude bulk oxidation rates for the waste pile. Subsequent to this, a numerical model that represents the coupled processes of heat and oxygen transport was developed for the site using the code TOUGH AMD. A vertical cross-section was used as the basis for a two-dimensional model and provided a coherent representation of the conditions within the pile and confirmation of the estimated physical properties. The Wismut database for the Nordhalde is unique in its scope and level of detail and provides insights into processes that likely occur in other waste piles in similar settings.

Key Words: Acid Rock Drainage, Oxygen Transport Processes, Waste Rock, Numerical Modelling

1.0 Introduction

Since 1992, SRK[1,2,3] has been assisting Wismut GmbH with their effort to rehabilitate the Ronnenburg mining district located in the former East Germany where extensive uranium mining was carried out between1946 and 1990 (Figure 1). The district is spread over an area of about 35 km^2 and comprises extensive underground workings, some 14 waste rock piles and a large open pit (the Lichtenberg Pit). A large portion of the rehabilitation effort has focused on the controlled relocation of mine waste to the Lichtenberg pit.

The Nordhalde (Figure 2) is the second largest waste pile in the district and forms the northwestern edge of the Lichtenberg pit. The pile stands approximately 70 m above the original ground surface at its crest, and contains some 27 Mm^3 of waste material. Two distinct materials form the pile. Acid generating material forms the largest portion of the dump volume and consists mainly of slates containing 1-2% pyrite. Typical seepage from this zone has a pH of about 2.7 and sulfate concentrations in excess of 10,000 mg/l. In some portions of the dump this material is overlain by non-acid generating material, or so called C-Zone material.
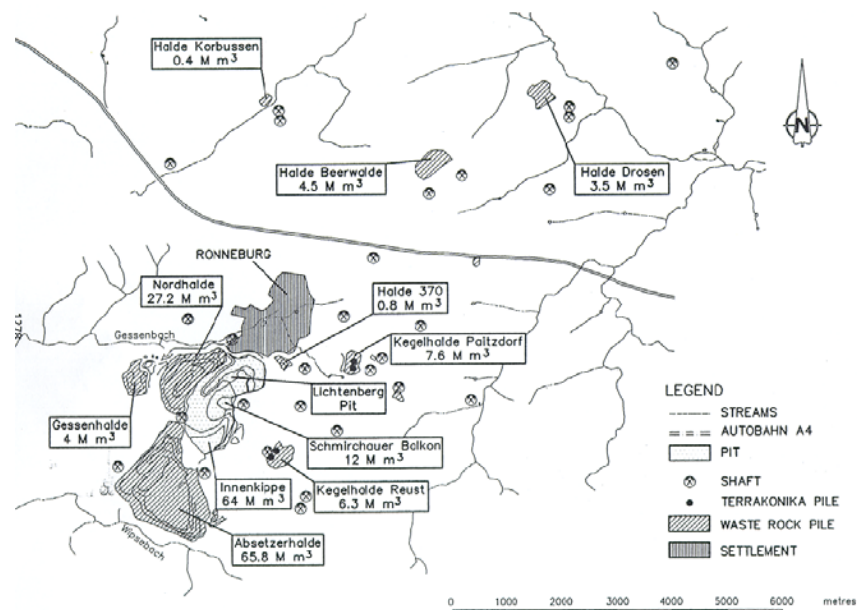
Figure 1. Map of The Ronnenburg Mining District.

During 1996 several remediation options were being considered for the Nordhalde warranting the installation of a system of gas, temperature and pressure monitoring devices to develop a better understanding of the oxidation processes leading to acidity generation within the pile. This paper summarises the observations from the monitoring program, subsequent analyses of the data and the coupled two-dimensional numerical model that was developed for the site.

2.0 Oxygen/Thermal Monitoring

Eight instrumented boreholes reaching depths between 8 and 75 m were installed during the summer and autumn of 1996 (Figure 2). The holes were situated to intersect areas with different acid generation and oxygen consumption potentials, and with different thicknesses of soil cover. Holes were drilled into the waste rock using a dry rotary air blast method and cased with 194 mm OD pipe. Instrumentation consisted of gas sampling and pressure monitoring tubes, thermistors and cables taped to the outside of 40 mm OD HDPE carrier pipe with the open tube ports and thermistors located at predetermined intervals along the length of the pipe. Filtercloth was wrapped around the assembly at the open tube port locations.

The instrumentations were inserted inside the casing to the bottom of the hole, centred at the collar and clamped into position. Backfilling of the borehole proceeded through a filling tube. Ports were backfilled with quartz sand and gravel separated by bentonite seals.

Temperature and pressure of all downhole monitoring ports were recorded hourly by means of automatic data loggers. Data from the pressure transducers lacked the appropriate sensitivity to be useful. Oxygen concentrations were measured manually on a daily basis (excluding weekends and holidays) using a Testo 346 Analyser. In addition to downhole monitoring, meteorological conditions (temperature, atmospheric pressure, windspeed and humidity) were recorded on a half-hourly basis from two reference stations at the site. At the time of the study, over one year of data had been collected from the installations. In terms of the internal oxygen and thermal conditions within a waste rock pile, the authors consider this data set to be one of the most comprehensive of its kind.
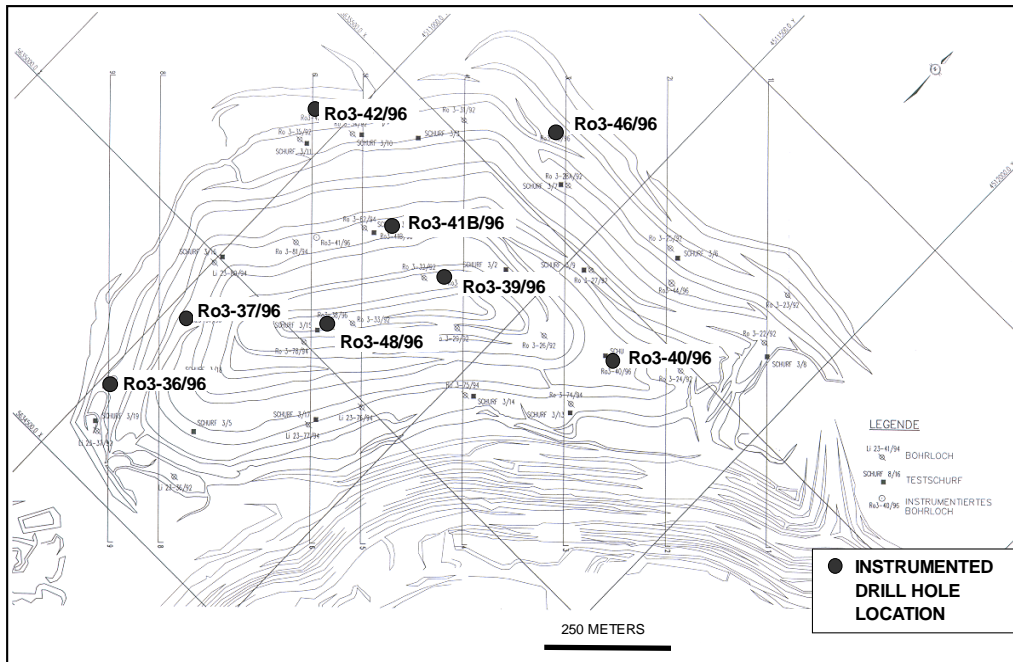
Figure 2. Instrumented drillhole location map.

3.0 Data Trends

Typical oxygen and temperature patterns are shown in Figures 3 and 4, which show monthly samplings of the profiles for Boreholes 36 and 38 respectively. Temperatures within these boreholes increase well above the annual average surface temperature of 8.5 ^{0}C, indicating active heat production resulting from exothermic pyrite oxidation.
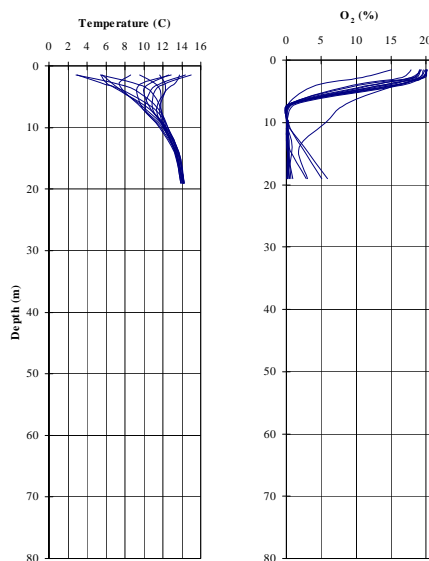

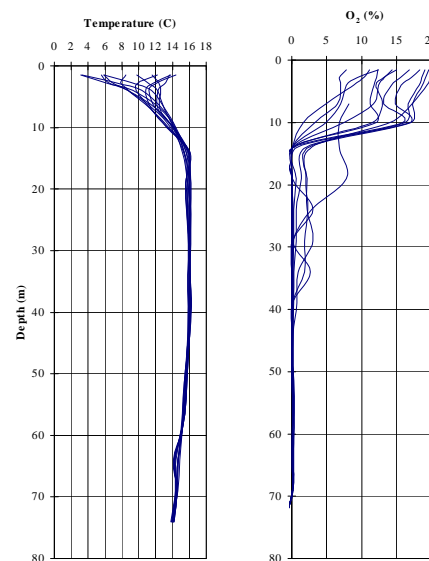Figure 3. Monthly sampling of temperature and oxygen profiles for Borehole 36.

Figure 4. Monthly sampling of temperature and oxygen profiles for Borehole 38.
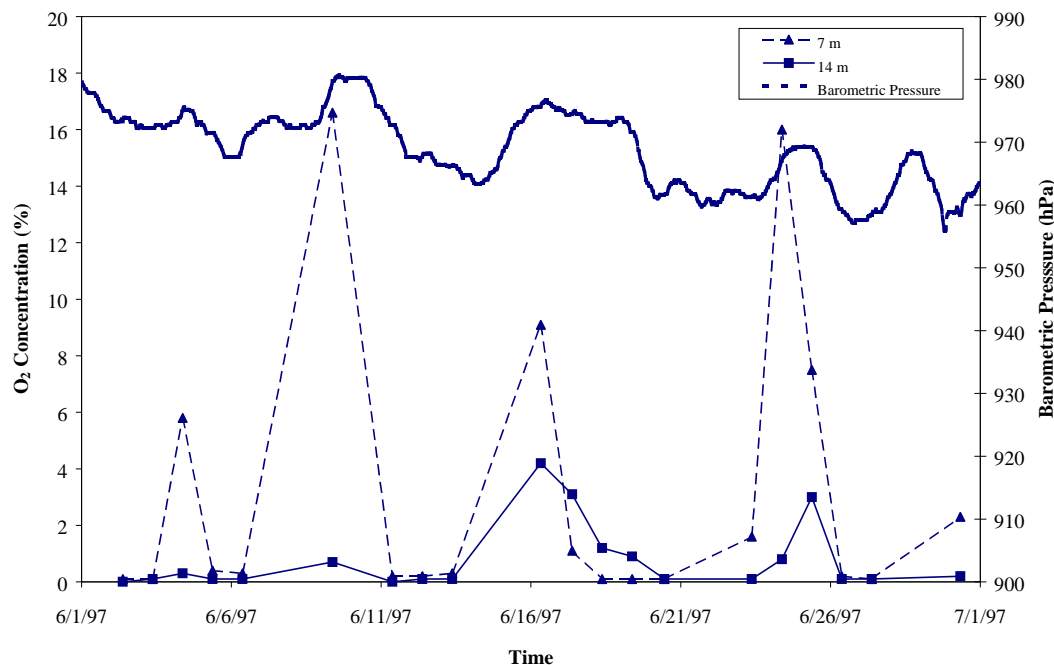
Figure 5. Fluctuations in oxygen concetrations and barometric pressure for Borehole 37.

Although the temperature profiles indicate the occurrence of pyrite oxidation, the oxygen profiles from these boreholes are more telling of the processes active throughout the year. During the summer months, diffusion is the dominant oxygen transport process, characterised by an exponential decrease in the oxygen concentration along the profile. Short-term changes in barometric pressure affect this pattern slightly, causing the profiles to shift upwards and downwards (Figure 5).

During the late autumn and early winter, when temperatures in the upper portions of the pile fall below the pile's internal temperature, the profiles show an overall increase in oxygen concentrations within the lower ports, indicating the onset of thermal convection (Figure 6). This pattern is most marked in the boreholes closer to the edge of the pile, where oxygen concentrations at depth remain high throughout the winter months. In boreholes towards the centre of the pile, oxygen concentrations in the deeper ports are more erratic, showing fluctuations of up to 15% O_2 over the period of one day. In all of the boreholes, the pattern of low oxygen concentrations at depth re-establishes during the late spring when temperatures within the upper portions of the pile once again rise above the internal temperature of the pile.

4.0 Preliminary Data Analysis

A preliminary quantitative analysis of the data was carried out to determine "order of magnitude" estimates of the bulk pyrite oxidation rate within the pile. For each borehole, independent estimates were obtained from the oxygen data and the temperature data.

The pyrite oxidation rate Q (Kg Pyrite $m^{-3} s^{-1}$) was determined from the temperature profiles using:

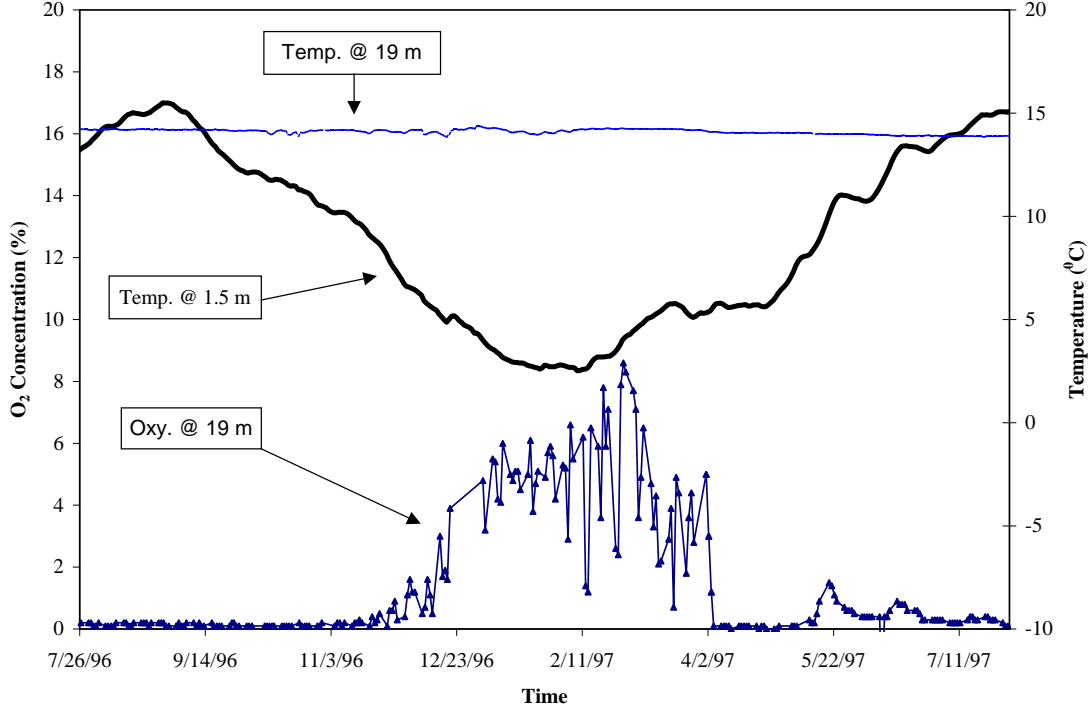$$Q = \frac{-k_t}{L}\frac{dT}{dz}R \qquad (1)$$

Figure 6. Relationship of oxygen concentrations in the 19 m port to temperatures in the 1.5 m and 19 m ports for Borehole 36.

Where k_t is the thermal conductivity (W m^{-1} ^{0}C^{-1}), dT/dz is the temperature gradient near the surface of the pile (^{0}C m^{-1}), R is the heat released from the oxidation of 1 kg of pyrite (11.7 MJ kg^{-1}), and L is the length of the borehole (m).

For this analysis, the thermal conductivity was estimated from:

$$k_t = \alpha C_v \qquad (2)$$

Where α is the thermal diffusivity (m^2 s^{-1}) and C_v (J m^{-3} ^{0}C^{-1}) is the volumetric heat capacity. Thermal diffusivity was obtained by matching observed temperature fluctuations in intervals of boreholes that did not contain heat sources to a one-dimensional heat conduction model. Volumetric heat capacity was estimated from the heat capacities of shale, water and air, and an assumed soil moisture content.

The above method assumes that heat production within the pile is due solely to pyrite oxidation and that heat loss from the pile occurs one-dimensionally through the surface. The annual average temperature profile for a borehole was used for estimating the temperature gradient. When a gradient towards the base of the pile was also evident (like in Borehole 36), the corresponding gradient was added to the gradient through the surface. Note that the oxidation rate calculated in this manner makes no attempt to identify the spatial distribution of heat sources within the pile.

275

A similar procedure was used for estimating the pyrite oxidation rate from the oxygen profiles. Assuming oxygen diffusion as the only oxygen transport mechanism, the volumetric oxidation rate was calculated using:

$$Q = -\frac{15}{4}\frac{D_{ox}}{M_{py}L}\frac{dC}{dz} \qquad (3)$$

Where D_{ox} is the oxygen diffusion coefficient for waste rock (m^2 s^{-1}), M_{py} is the molar mass of pyrite (0.120 Kg/mol), and dC/dZ is the oxygen concentration gradient near the pile's surface (mol m^{-4}). A value for D of $4x10^{-6}$ m^2/s was estimated from the literature. For this analysis, oxygen profiles from July 1997 were used to estimate the oxygen concentration gradient. Other oxygen transport processes, such as thermal convection and barometric pumping, were not accounted for in this analysis. Table 1 summarises the oxidation rates calculated by these two methods.

Table 1. Oxidation rates predicted from one-dimensional analysis.

Borehole	Oxidation Rate Predicted from Temperature Profiles (KgPy m^{-3}yr^{-1})	Oxidation Rate Predicted from Oxygen Profiles (KgPy m^{-3}yr^{-1})
Li 3-36	0.067	0.069
Li 3-37	0.052	0.023
Ro 3-38	0.029	0.019
Ro 3-39	0.028	0.0056
Ro 3-40	0.036	0.022
Ro 3-41b	0.040	0.022
Ro 3-42	0.34	0.24
Ro 3-43	0.19	0.20
Average	**0.098**	**0.075**

5.0 Numerical Modelling

Subsequent to the preliminary quantitative analysis of the data outlined above, a numerical model that represents the coupled processes of heat and oxygen transport was developed using the code TOUGH AMD[4]. The motivation for the modelling was to better understand the interaction of the multiple oxygen transport mechanisms and their impact on the bulk oxidation rate.

TOUGH AMD accounts for the coupled processes of multiphase heat and mass transfer for water, air and oxygen using an integral finite difference formulation. TOUGH AMD was developed from TOUGH2[5], a general-purpose multiphase non-isothermal numerical simulator. Oxygen is considered as a separate component from air to provide a link to pyrite oxidation. The model assumes a first-order rate constant for the kinetics of pyrite oxidation. A reaction core model provides the link between the surface reaction kinetics of pyrite oxidation and the volumetric oxidation rate. A more comprehensive description of the model, along with an application to the Mine Doyon waste dump in Quebec, is provided by Lefebvre and Gélinas[6], and Gélinas et.al.[7].

The model was developed as a vertical two-dimensional grid through a section of the dump containing both the A-Zone and the C-Zone (Figure 7) portions. A regular discretization of grid blocks 10 m high by 20 m wide was used for a total of 135 active elements. Fixed values of air pressure, water saturation (to set the infiltration rate) and oxygen concentration were imposed along the surface boundary (consisting of 41 non-active elements). A cyclic

boundary condition was used to represent yearly temperature fluctuations. In addition, some runs used variable pressure conditions at the boundary to study the effect of short-term barometric fluctuations. The bottom layer of active elements representing the waste rock (shown as Basal Blocks in Figure 9) allowed the calculation of heat loss using a semi-analytical solution adapted from a TOUGH2 module. A water saturation of unity was imposed along the base boundary (consisting of 9 non-active elements), and was assigned a very low value of heat conductivity to prevent any additional heat loss to them.

The parameters used for the model are summarised in Table 2. Many of these parameters were determined from an extensive physical and geochemical testing program of the Nordhalde, and a hydrological evaluation of the infiltration rates. Determination of the heat transfer properties is described in the preceding section. Vertical air permeability was determined by fitting pressure changes within the Nordhalde after a barometric event with an internal SRK model. Initial conditions for temperature and oxygen were set to 9^0C and 21% by volume respectively throughout the pile.

Table 2. Physical properties of the Nordhalde

| Property	Symbol and values
Global oxidation constant	$K_{ox} = 10^{-8}$ s^{-1}
Diffusive/Chemical times	$\tau_d/\tau_c = 0$
Pyrite mass fraction	$w_{py} = 0.031$
Horizontal permeability	$k_h = 8 \times 10^{-11}$ m^2
Vertical permeability	$k_v = 8 \times 10^{-12}$ m^2
Porosity	$n = 0.30$
Solids density	$\rho_s = 2751$ kg/m^3
Dry thermal conductivity	$K_{th,d} = 0.25$ W/m·°C
Wet thermal conductivity	$K_{th,w} = 1.2$ W/m·°C
Heat capacity of solids	$c_{ps} = 710$ J/kg·°C
Thermal conduct. of base	$K_{th} = 1,2$ W/m·°C
Global density of base	$\rho_b = 2106$ kg/m^3
Heat capacity of base	$c_p = 1021$ J/kg·°C
Standard diffusion coef.	$D_o = 4 \times 10^{-5}$ m^2/s
Temperature diffusion coef.	$\theta = 1.8$
Tortuosity factor	$\tau = 0.85$
van Genuchten m factor	$m = 0.256$
van Genuchten α factor	$\alpha = 0.00036$ Pa^{-1}
Residual water saturation	$S_{wr} = 0.284$
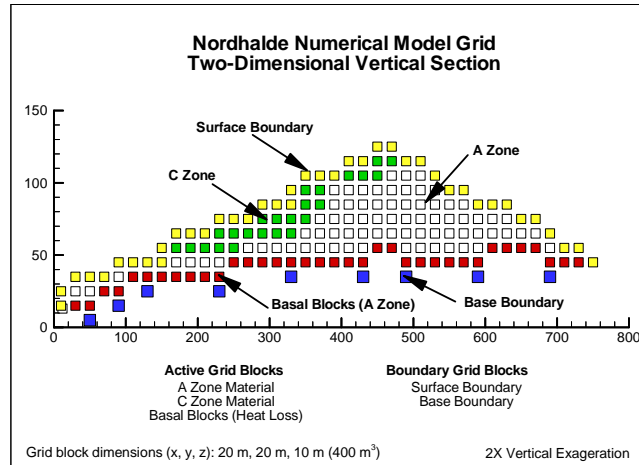
Figure 7. Grid used for the numerical model.

Figure 8 shows model results at the end of a 30-year simulation, corresponding to the period of operation for the Nordhalde. The model shows a significant increase in temperature from the initial condition, reaching nearly 20^0C at the core (Figure 8a), which is similar to the observed present day temperature within the pile. Gas velocity vectors show the occurrence of thermal convection, resulting in an average gas flux of 0.01 m/d through the pile in mid-February. Similar runs conducted with slightly lower values of horizontal permeability, did not allow the onset of thermal convection, resulting in much lower temperatures (about $12\ ^0$C) at the core of the pile after 30 years. The implication is that conditions in the Nordhalde exist near the limit between a wholly diffusive system and a diffusive-convective system. This conclusion is supported by the observed increase of thermal convection in the pile during the winter months.

Figure 8b shows higher oxygen concentrations near the pile's surface, reducing to a depleted zone at the core. Oxygen fluxes are mostly perpendicular to oxygen concentration contours implying that while convection occurs, diffusion remains the dominant supply mechanism. The higher oxygen fluxes that are observed on the edges of the pile relative to the top surface are explained by the upward convection of gas through the centre of the pile. This upward convection of gas with reduced oxygen content counteracts downward diffusion from the surface.
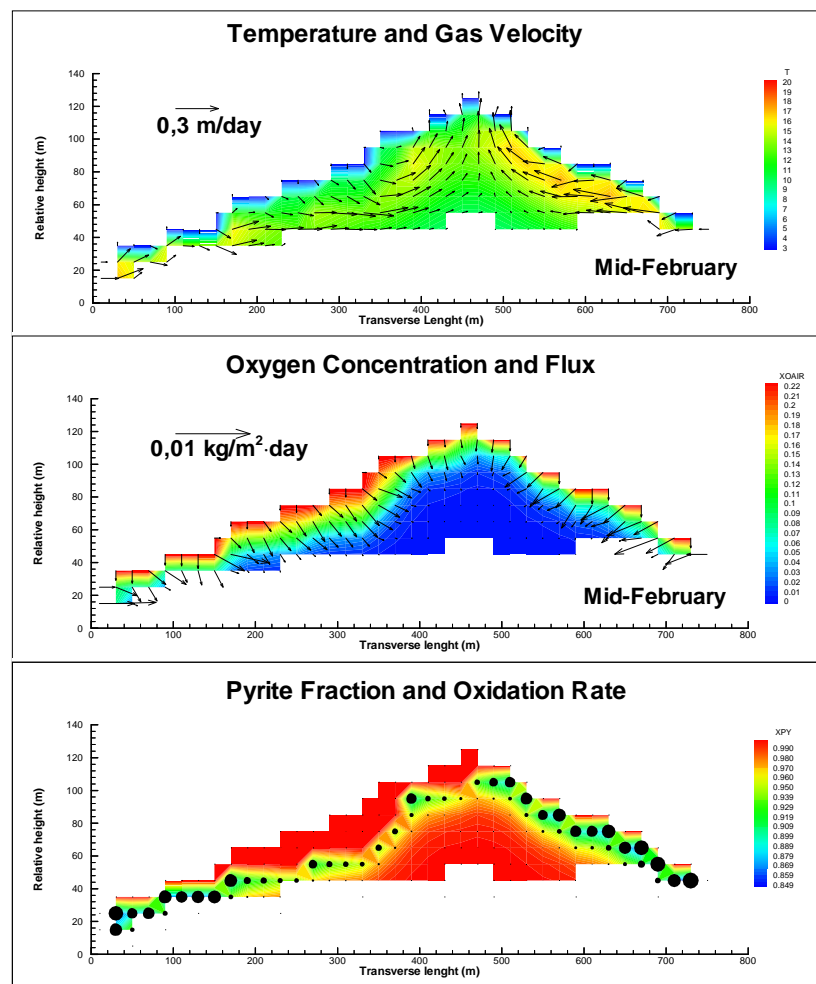

Figure 8. Model results after 30 years: a) Temperature and gas veolocity; b) Oxygen concentration and flux; c) Pyrite remaining and oxidation rate.

Figure 8c shows the effect of the non-acid generating C-Zone material on top of the pile. Lower temperatures and lower oxidation rates are encountered where C-Zone material is present. Figure 8c also shows slightly lower oxidation rates in the reactive material below the C-Zone material. This is due to the limited rate at which oxygen can diffusive through the C-Zone to react with the underlying acid generating material.
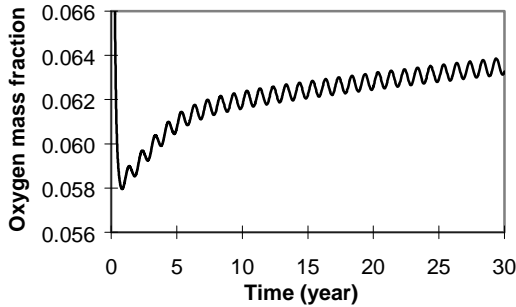

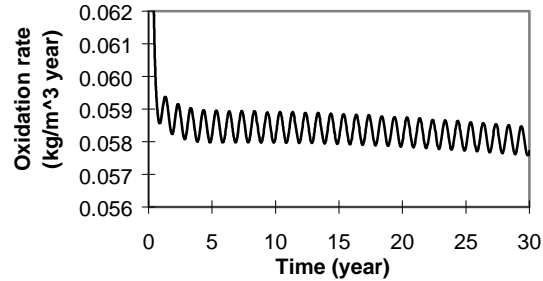Figure 9. Evolution of average oxygen concentration in the gas phase.

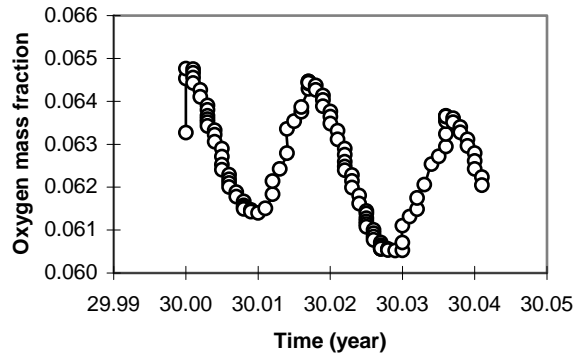Figure 10. Evolution of the average volumetric oxidation rate (in kg of O_2)

Figure 11. Modelled variations in oxygen concentration within the gas phase for barometric pressure changes.

Figures 9 shows the evolution of the oxygen mass fraction within the pile through the simulation. The cyclic effect that is superimposed onto the general trend is due to the seasonal expansion and contraction of gas within the pile caused by the induced cyclical temperature changes at the boundary. Further inspection of the trend reveals a break in slope beyond year 5, which occurs when the system goes from wholly diffusion dominated to one in which large scale convection plays a more important role.

The steady increase in the oxygen concentration shown in Figure 9 does not equate to a steady increase in the bulk oxidation rate. On the contrary, Figure 10 shows that at the end of the 30-year simulation the bulk oxidation rate is slowly decreasing with time. This is caused by the decrease in the reactivity of pyrite simulated by the reaction core model. TOUGH-AMD assumes that as readily accessible pyrite becomes depleted from the grain surfaces, an oxidised film builds around the pyrite grain resulting in a lower oxidation rate.

To study the effect of barometric pressure changes, a short-term modelling run was carried out using a variable pressure boundary condition. Initial conditions from the end of the previous 30-year simulation were used. Figure 11 shows that changes to barometric pressure result in short-term fluctuations in the overall oxygen concentrations within the pile, agreeing with the field observations. Further work is required to quantify this phenomenon's effect on the evolution of the bulk oxidation rate.

6.0 Conclusions

The Nordhalde provides a unique opportunity to enhance the understanding of the oxygen supply mechanisms that can occur in acid generating waste piles. The database for this site is exceptional in both quality and frequency of monitoring. The mathematical model reasonably matches the thermal and oxygen transport processes, implying that these processes are globally well described. The numerical modelling carried out in this study gives a better understanding of the processes that lead to thermal convection as well as the contribution of thermal convection to the bulk oxidation rate.

7.0 References

1. D.Hockley, M.Paul, J.Chapman, S.Jahn, W.Weise, Relocation of waste rock to The Lichtenberg Pit near Ronnenburg, Germany, in *Proc. 4th Int. Conf. On Acid Rock Drainage*, 1997, 1267-1301.

2. SRK (Canada) Ltd., Endbericht untersuchung der methoden für die in situe behandlung der Nordhalde und Innenkippe, SRK Report W104203 to Wismut GmbH, November 1995, 88 p.

3. SRK (Canada) Ltd., Endbericht teill III steuerungs-und kontrollprogramm, SRK Report W104108 to Wismut GmbH, March 1996, 64 p.

4. R.Lefebvre, Caractérisation et modélisation numérique du drainage minier acide dans les haldes de stériles, Ph.D. Thesis, Universite Laval, June 1994, 375 p.

5. K.Pruess, TOUGH2-A general purpose sumerical simulator for multiphase fluid and heat transfer, Lawrence Berkely Laboratory LBL-29400, 1991, 102 p.

6. R.Lefebvre and P.J.Gélinas, Numerical modelling of AMD production in waste rock dumps, in Sudbury '95, Conference on mining and the environment, May 28th-June 1, 1995, 869-878.

7. P.J.Gélinas, R.Lefebvre, M.Choquette, D.Isabel, J.Locat, R.Guay, Monitoring and modelling of acid mine drainage from waste rock dumps – La Mine Doyon case study, MEND Report GREGI 1994-12, 1994, 240 p.